Sensor for Small Satellite Relative PNT in Deep-Space

Josiah DeLange, Seth Frick, Joel Runnels, Demoz Gebre-Egziabher, Kale Hedstrom
University of Minnesota - Twin Cities, Department of Aerospace Engineering and Mechanics

***Abstract*—A prototype sensor designed to use of Gamma Ray Bursts (GRBs) as signals of opportunity for relative positioning, navigation and timing (PNT)in deep-space applications is described. GRBs are intense and aperiodic electromagnetic emissions which can last from a few fractions of a second to hours in length. What makes them suitable for navigation is that they are ubiquitous and can be sensed easily. The design of and results from laboratory testing of a prototype GRB sensor known as the Gamma Ray Burst Incidence Detector (GRID) is presented. Concept of operation for relative PNT using GRBs in CubeSat missions is also described.**

I. Introduction

This paper describes the development of a compact, low-cost gamma-ray detector which could be used for cooperative navigation and time synchronization among a fleet of spacecraft operating in an uncharacterized deep-space environment. The sensor described has the potential to enable gamma-ray based navigation, which would allow spacecraft to autonomously fix their position independent of Earth-based tracking. The sensor is both light-weight and inexpensive, meaning that it could be used as a navigation instrument aboard micro-satellites and other vehicles with severe size, weight, power and cost (SWAPc) constraints.

The remainder of this paper is organized as follows: In section II, the background and motivation for an alternative navigation sensor are discussed in context of the current methods for spacecraft PNT, particularly in deep space. This is followed by a conceptual overview of gamma ray burst navigation and how it originated. A short description of the motivation behind a small-form gamma ray detector in then given which is followed by a discussion of concept of operation for gamma-ray sensors including the basic equations used to estimate a position, navigation, and timing solution. A short discussion on sensing modality of gamma ray burst emissions is given by a detailed description of the software and hardware that comprise the gamma-ray sensor known as the Gamma Ray Incidence Detector (GRID). Some laboratory results for testing of the GRID sensor are presented. A summary and conclusion closes the paper.

II. Spacecraft Tracking

For spacecraft operating within close proximity of Earth, navigation solutions can be computed using various sensors including Global Satellite Navigation System (GNSS) such as GPS. These satellites reside in medium Earth orbit (MEO), roughly 26,000 km from Earth. However, there are numerous past, current and future envisioned missions beyond MEO, even beyond geosynchronous orbits (examples include past missions such as Voyager, Cassini, Galileo as well as current and future ones like MSL and MAVEN). Current position, navigation and timing (PNT) methods for spacecraft operating in deep space rely on ground and space-based tracking, in conjunction with optical navigation techniques. Moreover, PNT in space is heavily reliant on Earth-based tracking resources, in particular NASA's Deep Space Network (DSN), the largest and most sensitive telecommunications system in the world [1].

With the DSN, tracking is done with several key measurements. The Doppler shift of a spacecraft's coherent downlink carrier yields an estimate of the line-of-sight component of the spacecraft's velocity. Typically the precision could be on the order of fractions of millimeters per second, but this largely depends on the frequency of measurements. Additionally, there are uplinked ranging tones that measure an averaged distance to the spacecraft, given again that the update frequency is sufficient. This too is along the line-of-sight to the spacecraft. With the Doppler shift and average range, ground station operators will create ephemeris to enable acquisition and following of a given spacecraft.

Ground-based tracking via the DSN is capable of achieving high accuracy position solutions for objects in low-Earth orbit (LEO), but decrease in accuracy as distance from Earth increases. In addition, as more missions become dependent on the DSN (and as current spacecraft outlive their expected mission lifetime), the availability of DSN resources will become limited. Given the potential for increased CubeSat deployment, it is expected that many spacecraft will experience heavy delays in scheduling updates with the DSN. These could mean that satellites with a lower priority on the network would potentially see multiple days without updates. Further, beyond MEO the DSN is the only available source of man-made signal which can potentially offer measurements for a navigation estimator.

A navigation system which can operate independently of ground based range measurements is desirable because it both reduces the spacecraft's dependence on Earth-based tracking resources, and increases the accuracy of the navigation solution at large distances from Earth. It is possible that

spacecraft within the range of DSN may be able to update their position estimates from its ranging and Doppler measurements, however an additional subsystem capable of augmenting the DSN could offer a real benefit as missions travel farther beyond Earth. With growing efforts toward spacecraft miniaturization and increased potential for CubeSat deployment, it becomes costly and prohibitive to require vehicles to carry onboard the specialized active hardware for DSN two-way communication.

III. Gamma Ray Bursts

To deal with these challenges many proposals for navigation systems have been made. One proposed approach is to use signals from natural X-ray and gamma-ray sources as signals of opportunity that will allow relative (not absolute) navigation. One concept of operation that has been proposed is that of the "Mother-Daughter" ship scenario. The mother ship is a large and highly capable spacecraft located at a known position in space (e.g., a Lagrange point). The daughter ship or ships are smaller vehicle equipped with a sensor that can measure the signals emitted by a an X-ray or gamma ray source. The navigation solution becomes position of daughter ships relative to mother ship. Known X-ray pulsars, which theoretically can be identified uniquely by their periodic emissions, are in practice very weak/faint. We will not go into detail here about the challenges associated with using x-ray sources such as pulsars (most are related to SNR). Rather, we focus on high-energy celestial events known as gamma ray bursts (GRBs). GRBs are the brightest known electromagnetic events in the universe, and are thought to occur when a massive star in a distant galaxy collapses. [3] They are focused, high-energy, and high-photon count events, in contrast to the faint, low SNR X-ray emissions of a pulsar.

Gamma ray bursts were first detected in the late 1960s by U.S. military satellites designed to monitor covert nuclear testing. The *Velas* (Spanish for *"he/she watches over"*) were placed in very high orbits in pairs of two; when either detected a signature burst of gamma radiation, their observations were correlated to determine a location of the burst. After the first celestial gamma ray burst was observed in 1969 (and localized approximately on the FOV of the night sky), a paper was published from Los Alamos and research into the area of celestial gamma ray bursts developed over the following decades. There exists a network of orbiting observatories known collectively as the InterPlanetary Network (IPN). These in-space platforms have been in operation for over 30 years, providing triangulated GRB localizations from the burst time-of-arrival between the spacecraft. While there have been numerous iterations, currently the nine IPN spacecraft are Odyssey, Konus, RHESSI, INTEGRAL, SWIFT, MESSENGER, AGILE, and Fermi. In conjunction with the IPN is the Gamma-Ray Burst Coordinate Network (GCN), a ground-based network including optical and radio sites. The idea is to disseminate information quickly between observers. Knowing the position and attitude of each detector is what enables the burst localization.

Gamma-ray based navigation has been proposed as a means of estimating a spacecraft's position, in particular relative to other cooperating spacecraft [2]. Gamma-ray navigation falls into a larger class of opportunistic navigation methods, which attempt to extract navigation information from signals already existent in the operating environment. The model, essentially the inverse of the IPN, consists of estimating a relative navigation solution given the line-of-sight to a burst which is detected by several observers.

For the work described in this paper, it is assumed that the source of gamma-rays are GRBs. Being from a great distance, the resulting high-density flux of gamma photons released by an event arrives at our galaxy as a near-planar wavefront. The relative arrival times of these wavefronts at cooperating spacecraft could be used by these spacecraft to fix their positions relative to one another, and additionally to Earth, if the gamma-ray burst is also observed from Earth.

IV. Concept of Operation

The principle of using GRB for relative or absolute PNT was first outlined in [2]. In this section, we detail a relative positioning implementation for which the GRID sensor could hypothetically be used. In this navigation scheme, GRID would be used to make relative range measurements.

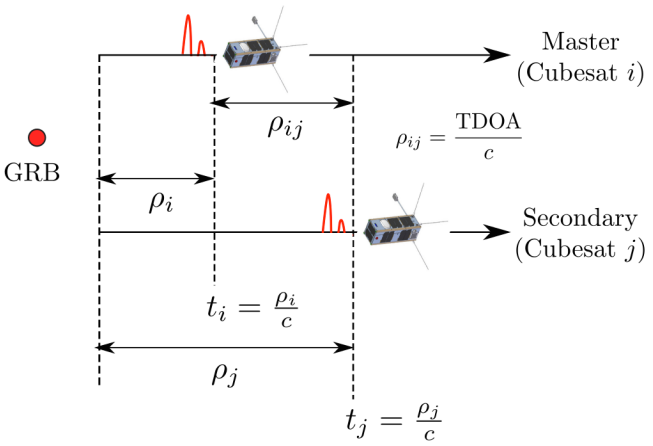

Fig. 1: GRB-based relative ranging concept.

This scenario is illustrated in Figure 1, where two small space vehicles designated as the master and secondary are able to exchange data via radio contact. They both observe a GRB event from a source located at a distance ρ_i away from the master and ρ_j away from the secondary space vehicle. Being equipped with gamma ray detectors, each vehicle will, as a result of the assumed GRB, detect at some point in time an influx of gamma ray photons (depicted as red pulses

in Figure 1). Having originated from the same progenitor, a particular pattern is realized by the master at $t = t_i$ and by the secondary at $t = t_j$. The estimated distance between the two space vehicles $\hat{\rho}_{ij}$ is related to the estimated time difference of arrival (TDOA) $\hat{t}_{ij}$ of the two respective burst realizations as follows:

$$\hat{t}_{ij} = \frac{\hat{\rho}_i - \hat{\rho}_j}{c} = \frac{\hat{\rho_{ij}}}{c} \tag{1}$$

where $c = 299,792,458 m/s$ is the speed of light in a vacuum. This is of course a simplified view of the problem because in addition to the Roemer delays t_i and t_j other effects (e.g., Shapiro or gravitational time delay) must be taken into account [5]. As far as signal processing goes, the delay is estimated with a correlation between observers. Often this method can be used under assumptions of superimposed uncorrelated noise, but we assume, given the lack of physical understanding of GRB progenitors, that it is not well-supported scientifically to assume a burst detection can be separated from superimposed background environment. For what we are demonstrating with the GRID sensor package, the assumed burst is detectable by identical GRID sensors, which will detect signals which illustrate independent, spatially separated realizations of the stochastic process which causes the influx of photons (the GRB).

Time integrated photon counts can be easily produced with an "accumulate-reset" scheme (to produce the red pulses of Figure 1 as time-dependent photon counts), however the correlator accuracy begins to suffer as time resolution is increased, i.e., for narrow accumulation periods, due to its heavy dependence on signal-to-noise ratio (SNR). This issue is discussed further into the paper. Supposing though that the number of photons produced by the burst is sufficiently high (which is possible for some GRBs with estimated emissions up to 1000 photons/sec/keV), higher temporal resolution measurements will see a slight improvement in SNR. For these types of bursts, we can immediately see from (1) the need for high temporal resolution in the gamma-ray detectors used for computing a navigation solution. Suppose that the detectors used are capable of measuring the arrivals of gamma-ray bursts with a temporal resolution of τ. Then the highest spatial resolution we can hope to achieve from such a detector, is $c\tau$. For instance, if the detector's time resolution is 10^{-6} seconds, then the best spatial resolution achievable from this detector would be 300 meters. Note that this limitation may be mitigated in post-processing.

When directionality and clock errors are introduced, the problem can be represented as shown in Figure 2. Assuming that n different GRBs are being observed (not necessarily simultaneously) then the relationship between the n^{th} GRB signal and the relative PNT between the two space vehicles is as shown in Figure 2. If the unit line-of-sight vectors pointing in the direction of the GRB from the master and secondary spacecraft are $l_i^{(n)}$ and $l_j^{(n)}$, respectively, then the n^{th} GRB signal TDOA $t_{ij}^{(n)}$ is related to the relative range ρ_{ij} by:

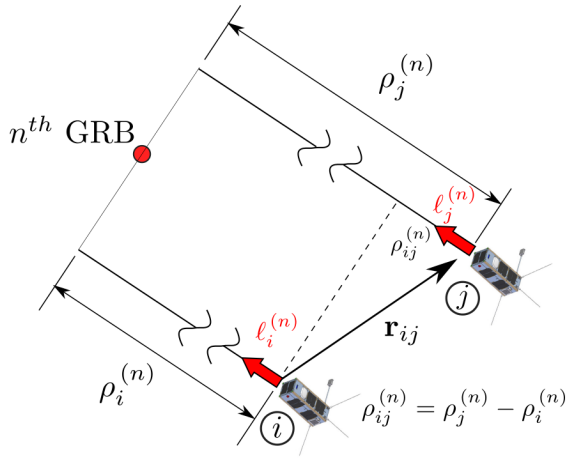

Fig. 2: GRB-based 3-dimensional positioning and timing

$$t_{ij}^{(n)} = \frac{\rho_{ij}}{c} + \delta t_{ij} = -\frac{(l_i^{(n)})^T \boldsymbol{r}_{ij}}{c} + \delta t_{ij} \tag{2}$$

where $\boldsymbol{r}_{ij}$ is the relative position vector between the space vehicles; δt_{ij} is the clock offset between the master and secondary spacecraft; and we have assumed that the source of the GRBs are very far away implying $l_i^{(n)} = l_j^{(n)}$ Thus, for $n \geq 4$ the three components of the relative position vector $\boldsymbol{r}_{ij}$ and the clock offset δt_{ij} can be estimated. This is effectively the same equation as the GNSS position fixing problem. [6]

Clock errors thus become extremely important for the GRID sensor package. The clock error is the offset between the master's and the secondary's clocks. One of the purposes of GRID is to estimate this clock offset and, thus synchronize the timing between the two space vehicles. In particular the clock delay will have to be decomposed in various components. Some of these components are going to be a function of the quality of the clocks used on both CubeSats. Many of the errors are going to be stochastic in nature, requiring the estimation of $\boldsymbol{r}_{ij}$ and δt_{ij}. However, in this paper we will focus exclusively on our work developing measurement hardware allowing for the estimation of t_{ij} by methods involving cross correlation. For this reason the onboard clocks are assumed to be highly precise chip-scale atomic clocks (CSACs).

As shown in Figure 2, GRID will allow two spacecraft to know their location relative to one another. A general overview of the scenario we are investigating is the following: consider the two CubeSats shown in Figure 2. Each CubeSat is equipped with a GRID sensor. Each will make an observation of a GRB (or any other x-ray or gamma ray emission). They will time-tag the observation using their onboard clocks. The result of this measurement will be a light-curve with specific features that can be correlated between measurements. The master's light curve (or a compressed version of it) will be

broadcast to the other spacecraft. By using the master's light curve and correlating it with a similar light curve measured onboard, the space vehicle may estimate the time-difference-of-arrival (TDOA) of the observed GRB photon fluxes. This forms the basic observable that is used in the PNT solution. Then, given four or more TDOAs, a spacecraft can estimate its relative position relative to the master.

Small satellites containing a GRID sensor are therefore equipped for an increased level of autonomy when traveling into deep space, especially given that the DSN is actively looking for ways to load-shed subscription burden. On the user end (spacecraft), each update costs money and spacecraft resources (power, time, memory, etc.). On the DSN side, each update has to be scheduled and slots are increasingly limited. Given that GRBs can occur randomly from any given direction, as is generalized in Figure 2, the scenario we are describing could provide additional axes of position determination. The DSN only gives range and range rate along the line-of-sight from ground station to the spacecraft; it does not give the transverse position, and accuracy in the two transverse axes is reduced. GRID enables a method of reducing the subscription burden and increasing accuracy of position via updates for the transverse axes. (One example scenario would be where a spacecraft's LOS to the DSN antennas is obstructed by a planetary body.)

V. Gamma Ray Sensing Modality

Gamma ray bursts are picked up by what is referred to as the detector assembly. The detector assembly refers to the sensor head, which stops gamma ray photons and converts their energy either into light, in the case of a scintillator, or an electrical pulse, in the case of a solid-state detector. In the case of a scintillator, the sensor head also includes a device (phototube, photodiode, or avalanche photodiode) which converts the scintillation light into an electrical pulse. The two practical choices for GRID's sensor head were 1) inorganic scintillators and 2) solid-state detector arrays. Both of these have been well-tested and used frequently in space missions involving flux measurement and gamma spectroscopy.

A. Inorganic Scintillators

Scintillators operate by converting incident energy into scintillation light. The mechanics of scintillation can be described by the "energy gap" model. Energy deposited into an inorganic scintillator displaces charge carriers within the crystal; these excitations "jump up" from the valence band into the conduction band. It is during their subsequent relaxation to their ground state that luminescence occurs. Different impurities instill additional energy states between the exciton band and valence band (thus producing more scintillation photons). It is also during this process that some excitons do not make it back to the valence band, and are trapped, therefore releasing no scintillation photons. The energy is dissipated elsewhere, and no sensing can occur. Dopants, which help reduce the statistical probability of trapping, also increase luminescence to near-theoretical limits. Additionally, different dopants result in unique emission characteristics (e.g. wavelengths and light intensity decay constants), leading to practical and impractical choices of optical readout systems for unique detector materials.

B. Solid State Detectors

Cadmium-Zinc-Telluride (CZT) has been used in several space applications that are roughly similar to what GRID is proposing. The SWIFT mission uses an array of 40,000 CZT detectors, as well as the NuSTAR mission. Its advantages are good stopping power, low energy thresholds down to about 15 keV, and excellent energy resolution. Its main disadvantage is that it is only available in small sizes; this means that an array would be required for our application. A description of an array for planetary gamma-ray spectroscopy can be found in [4]. In contrast, the GRID equivalent of the CZT array would not require the bismuth germanium oxide (BGO) anticoincidence described in this paper. CZT is denser than CsI(Tl) (5.78 g/cm^3 vs. 4.51 g/cm^3) less sensor would theoretically provide an equivalent stopping power. CZT crystals are often bonded to printed circuit boards which contain a charge-sensitive preamplifier, very similar to the readout system of GRID, but more self-contained. However, CZT arrays are expensive, and also require a slightly higher bias voltage, and are susceptible to pulse pile-up during high-rate environments.

VI. Gamma Ray Incidence Detector (GRID) prototype

Current gamma-ray burst detector assemblies, for example SWIFT and HXT, are massive, large area instruments. Many of these detector assemblies are designed for a high energy resolution, but not for applications requiring high timing resolution. Our design seeks to focus on a detector assembly which enables the t_{ij} between two detectors to be measured. Additionally, given the estimated increase in CubeSat deployment, our design focuses on integration into a CubeSat platform. To address these specific CubeSat (or miniature satellite) needs for gamma-ray navigation purposes, the GRID detector has been designed with three general design constraints: small size, low cost, and high temporal resolution. GRID is a proven prototype which aims to provide an additional means of increasing CubeSat autonomy. While certain astronomical observatories are currently in use, monitoring X-ray and gamma-ray emission from outer space, none have been designed to 1) record gamma-ray bursts with the temporal resolution needed to achieve a high-resolution navigation solution or 2) utilize miniaturized space vehicles. So, what we seek to determine is how to design a CubeSat-ready gamma-ray PNT sensor.

Further, we seek to investigate various aspects of the design, as well as trade-offs affecting its performance as a PNT sensor.

GRID was optimized to 1) detect the maximum number of GRBs and 2) gather the maximum number of photons for each GRB, given the following constraints: 1) a volume less than or equal to one CubeSat unit and 2) a mass less than or equal to one-third the mass of a 3U CubeSat. The first requirement to detect the maximum number of GRBs implies maximizing the sensor head area, given the proper optical readout system. The second requirement to detect the maximum number of photons for each GRB is accomplished by designing for a lower energy threshold (under 100 keV). Additionally, other derived requirements were intended to reduce the systematic uncertainties associated with comparison of GRB time histories from two detectors. GRID's detectors were required to achieve good energy resolution and assumed a pulse gain, i.e. pulse height vs. energy, which is stable or calibrated (or able to be post-processed).

A photograph of the prototype is shown in Figure 3. It is a proof-of-concept GRB sensor head with readout electronics, consisting of a detector housing containing four crystal sensing elements. The sensing elements are located below a carbon composite window which can be seen clearly on the top of GRID, in the photograph of Figure 3. We considered the CsI(Tl) and avalanche photodiode (APD) combination as the best choice for gamma detectors. An APD offers a greatly reduced volume for roughly the same method of operation as a PMT (at a lower bias voltage also). Detection materials such as BGO (SWIFT and FERMI include BGO detectors to stop high-energy gammas), and organic (plastic) scintillators were not included as potential design choices. BGO does not achieve a low energy threshold due to its low light output, and organic scintillators have a low photopeak efficiency (implying a poor effective energy resolution). CsI(Tl) shares many similar properties to CsI(Na), which has been used widely in space applications. It is easy to machine, rugged, and has a good light output well-matched to APD-sensitive wavelengths. Figure 5 shows shows the sensing elements when the carbon composite gamma window is removed. Note the gamma window is not required for GRID to be omnidirectional; it was designed as a back-up method to enable directional hard X-ray measurements from pulsars during the test flight. This is not discussed in this paper, however.

The readout electronics of GRID's first prototype have been designed specifically to conform to the PC/104 embedded computer standard, requiring only power rails on the PC/104 bus. The PCB layouts are thus able to migrated to CubeSat platforms with minimal mechanical interference or compatibility issues. It has been integrated into a PC/104 stack and flown on a high-altitude ballooning flight to gain flight heritage [5]. In what follows key elements of the detector are described in detail.

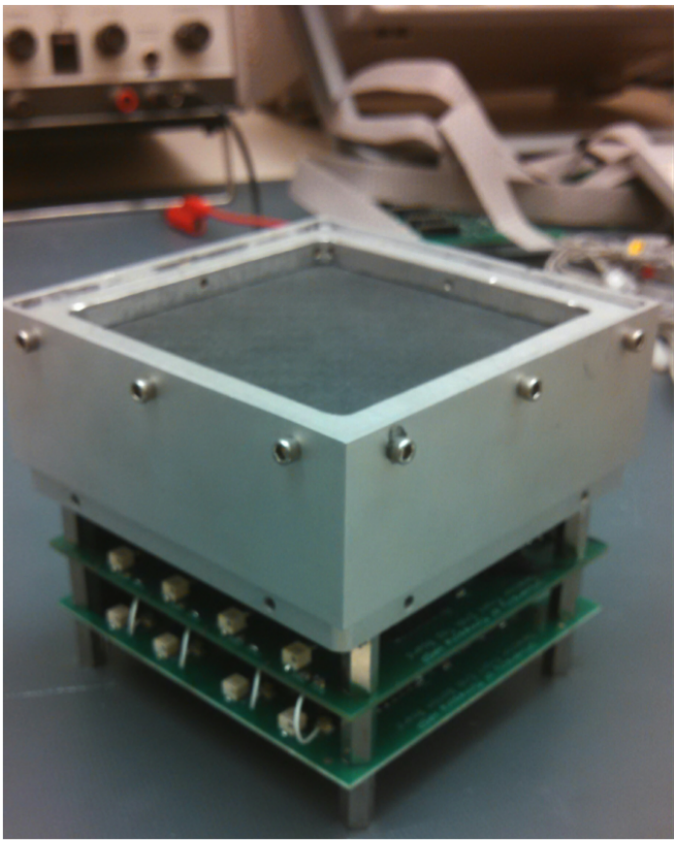

Fig. 3: The GRID sensor head, shown with carbon composite gamma window (top) and readout electronics.

A. Gamma Ray Sensor Head

A dimensional drawing of the GRID sensor head is shown in Figure 4 which consists of the four CsI(Tl) scintillation crystals their mechanical support structure. A photograph of the crystals in their support housing is shown in Figure 5. Each crystal is a 2cm x 2cm x 4cm block. Their light emission is nearly linear, typically around 54 photons / keV at a wavelength of 550 $\pm$ 200 nm, and the scintillation time on average is estimated to be close to 1 μs. The sensing elements are wrapped in a white polytetrafluoroethylene (PTFE) tape, wrapped in tape on lateral faces and surrounded by shock-resistant foam and silicone, and housed in individual optically decoupled cavities. By using four detectors, detection area was maximized, while minimizing the optical readout's volume and power. Attached to each CsI(Tl) crystal is an 5x5 mm Hamamatsu S8-664-55K short wavelength type avalanche photodiode (APD) [7]. The APDs convert the light created from the interaction of gamma-ray photons with the CsI(Tl) crystal to an electrical pulse. Typical photosensitivity is 0.24 A/W, peaking at wavelength 600 $\pm$ 200 nm. Each is affixed to a CsI(Tl) crystal using a translucent optical adhesive which acts as a light guide. The APDs require a 300 VDC bias, produced by a high voltage supply board contains two voltage multipliers, each driven by a 12 VDC power rail. The prototype used during flight testing was located farther

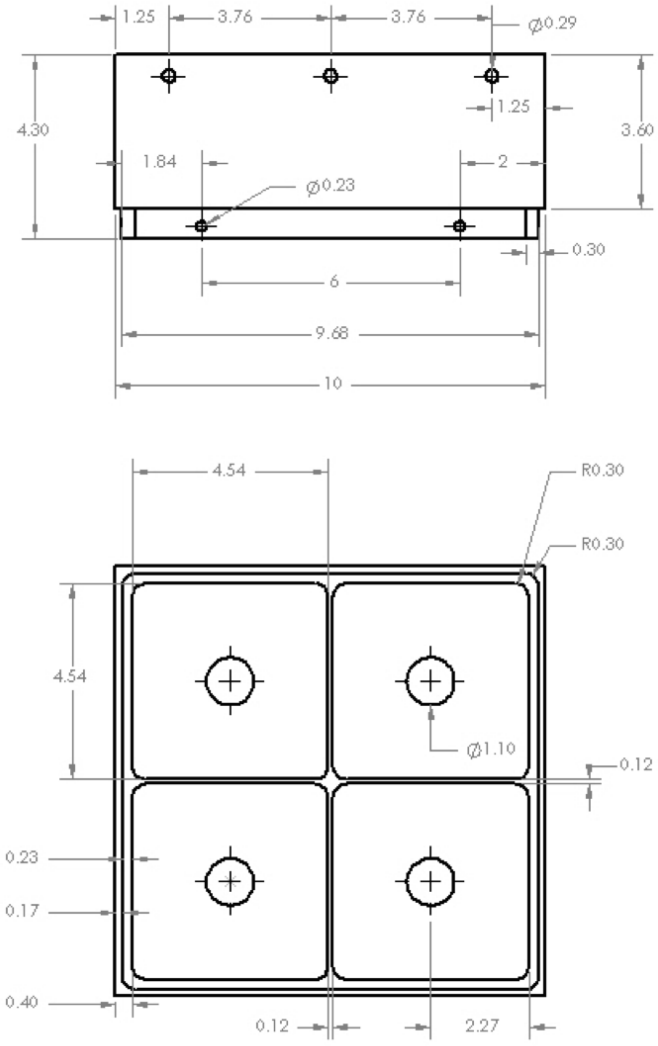

Fig. 4: Dimensions (centimeters) of the GRID sensor head housing.

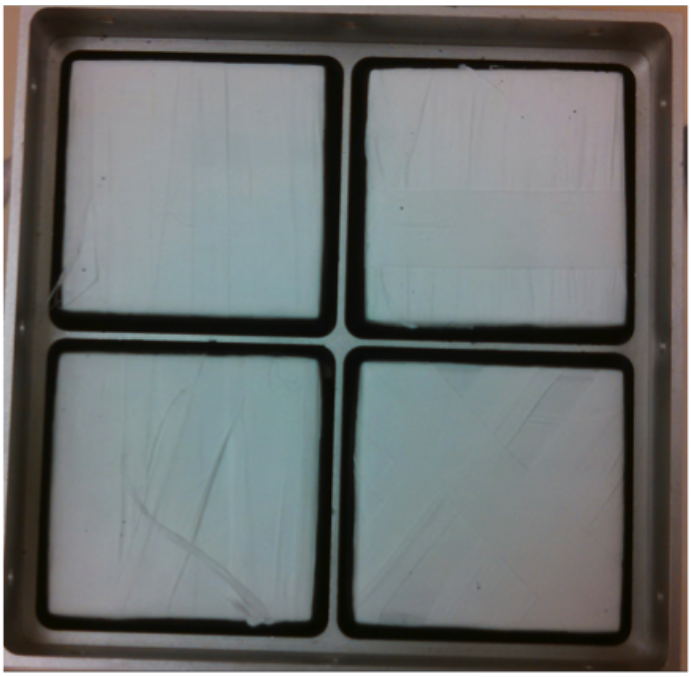

Fig. 5: Top view (uncovered) of the GRID sensor head showing the four (wrapped) CsI(Tl) detectors.

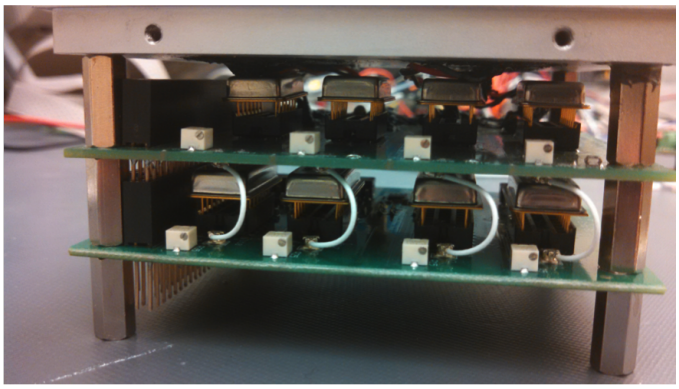

Fig. 6: GRID's readout electronics, located directly under the housing.

down in the stack. Keeping this away from the sensor head minimizes the interaction between switching transformers and the sensitive readout electronics. Four sets of APD leads are fed through holes in the bottom of the housing to the electronic readout, located directly below the housing.

B. Readout Electronics

A photography of the GRID readout electronics is shown in Figure 6 and consists of two printed circuit boards (PCBs) using four sets of of hybrid integrated circuits from Amptek, Inc. These are the A-225 preamplifier/shaping amplifier and the A-206 shaping amplifier/discriminator. In conjunction, these produce constant-frequency electrical signals from the APDs viewing the detectors, with amplitudes indicative of the relative intensity of scintillation light. The first-generation design of the readout implements a track-and-hold peak detector circuit, which holds the pulse height constant until it is able to be subsequently sampled by an analog-to-digital converter. Trimpot voltage dividers on the PCBs allow an adjustable (sub-unity) pulse gain and an adjustable detection threshold. This allows GRID to be calibrated with respect to spectral lines and to the "noise floor" of resolvable pulse amplitudes. In other words, each detector of GRID can be calibrated to observe different energy bands. The system dead time is on the order of tens of microseconds, and is a combination of scintillation light decay time (1-2 μs) and pulse shaping (6-7 μs). Four A-225 preamplifiers are housed on the first board and four A-206 amplifiers are housed on the second. Signals are passed by the miniature coaxial cables seen in Figure 6. In summation: two electrical signals are available (per channel) of GRID: the discriminator signal,

used for gated logic, is taken to represent the particle's time-of-arrival (TOA). The pulse height, i.e., peak voltage, is taken as the relative energy of an incident particle.

VII. Performance of GRID

A. Detectors

Individual detectors were calibrated via irradiation with calibrated sources in the laboratory, with energies ranging from 75 keV to 1.33 MeV. The experimental setup consisted of a prepared detector crystal and radioactive source placed into a light-proof aluminum box, with APD leads soldered to a coaxial BNC cable. The signal from the APD was fed through an amplifier board using the same A225/A206 circuit described above. The resulting analog pulses (discriminators and pulse heights) were within the 1-10V range and fed into an Ortec EASY-MCA multichannel analyzer (MCA). The MCA produced pulse-height spectra which are used to characterize the CsI(Tl) detector's energy resolution. Radioactive samples used were ^{137}Cs (0.662 MeV), ^{60}Co (1.17 MeV, 1.33 MeV), and ^{232}Th (238.63 keV). The Full Width at Half Maximum (FWHM) energy resolution of the CsI(Tl) detectors is:

- 2% Full Width at Half Maximum (FWHM) @ 238.63 keV
- 13% FWHM @ 662 keV
- 6.8% FWHM @ 1170 keV
- 6.8% FWHM @ 1330 keV

Light produced in a scintillator crystal is generally linearly proportional to deposited energy for high energy particles like hard X-rays or gamma rays. However, for low-energy interactions, there may be significant non-linearity. [11] The experimental goals were to measure energy-channel relations, and angular responses. However the small size of the detector limited the strength of conclusions made. Future tests, if able to incorporate higher-grade sources and testing equipment, may be able to further characterize the detector performance in spectroscopic applications.

B. Flux Response

Note that it is extremely difficult to simulate gamma ray bursts in most settings. We evaluate the performance of the detector by simulating several photon fluxes in the laboratory. First, the background count rates were observed in the laboratory setting, in the absence of all radioactive samples. This varied by detector as follows:

- Detector 1: 4.3779 $\pm$ 4.1942 cts/sec
- Detector 2: 6.6906 $\pm$ 6.7693 cts/sec
- Detector 3: 3.8950 $\pm$ 3.9570 cts/sec
- Detector 4: 2.0765 $\pm$ 2.0981 cts/sec

A sample of ^{232}Th (90 keV to 911 keV) is briefly unshielded, then re-shielded, producing signals (above the background rates) at the detector similar to that of a gamma ray burst. We used a custom-designed data processing unit (DPU) to produce TOA datasets. The prototype DPU was designed initially for the high-altitude balloon flight, and uses several microcontrollers, a 16 MHz oscillator, and an OEMStar GNSS receiver to produce precise timestamps for detected particles. These timestamps were derived from the GPS pulse-per-second and the 16 MHz oscillator, for a temporal resolution of 1 μs. For ground-based testing, clock drift was very low.

C. Cross Correlation

The result of this architecture is a dataset which can be thought of as a vector of timestamps $\{t_1, t_2, t_3, ...t_M\}$, where the timestamps are increasing in order. This allows a similar derivation to the XNAV formulas used in [8] where the measurement model has the following form:

$$\begin{aligned} y_1(t) &= y_b^{(1)}(t) + h_1(\lambda(t)) \\ y_2(t) &= y_b^{(2)}(t) + h_2(\lambda(t-\tau)), \end{aligned} \tag{3}$$

where $y_1(t)$ and $y_2(t)$ are the aggregate count rates at two spatially separated detectors. We model the count-rates of the two detectors as the sum of two processes: the background noise observed by the detectors, $y_b^{(1)}(t)$ and $y_b^{(2)}(t)$, and the photon counts produced by the gamma-ray source $h_1(\lambda(t))$, and $h_2(\lambda(t-\tau))$.

Note in particular the notation of $h_1(\lambda(t))$. This notation is chosen to indicate that each light curve h is assumed to be an independent realization of a random Poisson process, for which the underlying parameter is a function of time, $\lambda(t)$. The underlying parameter $\lambda(t)$ is the expected number of photons per second, and is directly proportional to the photon flux and size of the detector. This parameter, $\lambda(t)$, can be assumed to be the same at each detector, with the exception of the time offset due to the spatial separation between the two detectors. Therefore, $\lambda(t)$ is the parameter of interest for estimating the distance between the two detectors. If the values of $\lambda(t)$ are sufficiently large, or equivalently, if the accumulation period is sufficiently long, then the parameter $\lambda(t)$ may be estimated at each time period as the number of photons counted during that period divided by the length of the time bin, i.e.

$$\lambda(t_i) \approx \frac{y(t_i)}{\Delta t} - \hat{y}_b \tag{4}$$

where $y(t_i)$ is the number of photons counted during time bin i, and τ is the width of that time bin in seconds and $\hat{y}_b$ is an estimate of the background count, estimated before the arrival of the burst.

Under this assumption, we approximate $h(\lambda(t)) \approx h_1(t) \approx h_2(t)$ (implying $h(t)$ is a unique function observed at each detector at times separated by delay τ). Also, here the background noise consists of additive Poisson noise sequences, captured by the background count rates $y_b^{(1)}(t)$ and $y_b^{(2)}(t)$ at each detector. (These assumptions, used only in the scope of laboratory testing, are supported by the measured background

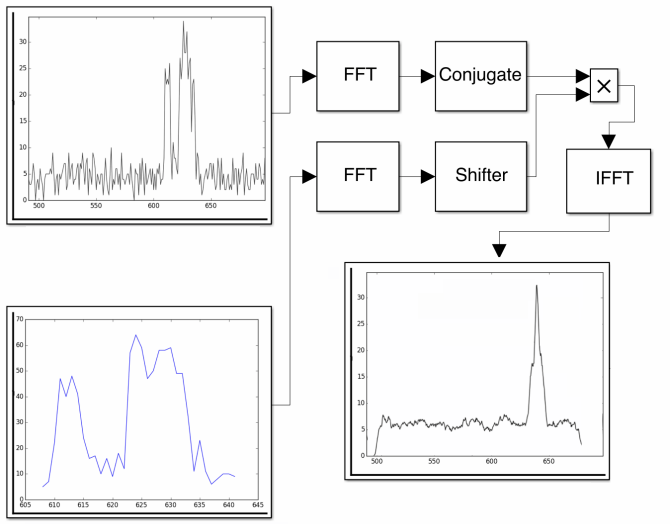

Fig. 7: Cross correlation architecture using the Fast Fourier Transform (FFT).

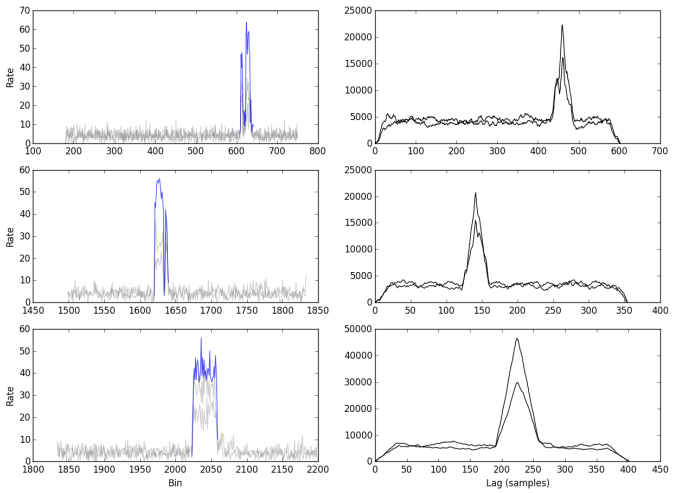

Fig. 8: Three simulated photon bursts measured by GRID (left) and the resulting cross correlation between GRID's detectors (right).

count rates.) The normalized cross-correlation $R_{12}(\tau)$ between $y_1(t)$ and $y_2(t)$ is given by

$$R_{12} = \frac{1}{N_s} \sum_{k=1}^{N_s} y_1[k] y_2[k-\tau] \tag{5}$$

where N_s is the total number of samples, or time bins. The most likely estimate of TDOA, $\hat{\tau}$, is then

$$\hat{\tau} = argmax[R_{12}(\tau)], \tag{6}$$

the value of τ which maximizes the cross correlation function $R(\tau)$. For the purposes of GRID's concept of operation, the projected distance between spacecraft becomes $\hat{\tau}c$, where c is 299,792,458 m/s in a vacuum, ignoring other more complex relativistic effects. Note that in lieu of high-resolution time binning (implying more samples around the cross correlation function's peak), other mathematical approximations involving peak fitting have been used to quantify correlation accuracy. [10], [12]. The software architecture used for cross correlation is shown in Figure 7, and was implemented in post processing.

Each detector of GRID is independent from the others (because GRID only processes one detector at a time). Therefore, for a given high-flux event, correlation between detectors of GRID can give a rough estimate of the inherent statistical uncertainty of the method. Figure 8 illustrates this for photon counts measured by GRID during artificially-induced fluxes. In theory, correlator accuracy is lower for high SNR signals. (We will not discuss this in great detail.) To estimate $\hat{t_{ij}}$, our detector assembly is capable of measuring time integrated photon counts parameterized by the accumulation period. For the laboratory simulations plotted in Figure 8, the accumulation period was one second and the resulting cross correlations achieve accuracies (in terms of peak spread) on the order of milliseconds.

VIII. Results and Conclusions

During laboratory testing, GRID suggests a correlation accuracy corresponding to several hundred kilometers of accuracy for $\hat{\rho_{ij}}$. Given the heavy dependence on SNR, results from laboratory testing (est. up to 20 photons/second/keV) may be considered a conservative estimate for GRID's flux response to high-photon events like GRBs. The correlation function is very sparse for low-count signals, introducing significant uncertainty in $\hat{\rho_{ij}}$. Conversely, the correlation can work quite well when photon fluxes are sufficiently high. Given this conservative estimate of $\hat{\rho_{ij}}$ (accurate to a few hundred kilometers), GRID can potentially offer a method by which small satellites in deep space are able to, in communication with each other, estimate relative ranges. This may become increasingly useful as missions travel farther from the Earth. More generally, we have demonstrated that gamma ray bursts could be potentially used for relative navigation and timing applications aboard a fleet of cooperating spacecraft. What we have shown in particular is the hardware design of a prototype sensor which enables small satellites to measure gamma ray bursts. Using the GRID sensor package, a fleet of small spacecraft monitoring gamma-ray emissions can therefore estimate their relative positions and clock offsets as we have shown. Given the increased potential for CubeSat deployment, such the ideal sensor would be small enough, light-weight enough, and inexpensive enough to be incorporated into micro or nano satellites. The design which we have described for the GRID sensor package, illustrates the result of these requirements: a working prototype of a gamma ray burst PNT sensor, for CubeSats, with a time resolution sufficient for TDOA estimation.

IX. Future Work

Currently two CubeSats projects are underway to test GRID in LEO. The first of these projects, Experiments for X-ray Characterization and Timing (EXACT) is sponsored by the USAF University Nanosat Program. The second project, Signal of Opportunity CubeSat Ranging and Timing Experiments (SOCRATES) is sponsored by NASA's University Student Instrument Program (USIP). EXACT and SOCRATES are identical CubeSats. If launched simultaneously, then the will be used to characterize GRID performing an experiment akin to what is depicted in Figures 1 and 2. If schedule do not permit the CubeSats to be lanuched individually, they can still be used to validate GRID's performance along the lines of the validation experiment illustrated in Figure 9. Once in orbit, the GRID sensor on EXACT or SOCRATES will be able to make photon flux measurements to detect GRBs. When photons from GRBs are observed, the photon measurements will be time-tagged and recorded. Simultaneously, other gamma-ray burst observatories, such as the *SWIFT* spacecraft and the *Fermi* gamma-ray burst monitor also measure gamma-ray bursts. The data from these observatories are made publicly available shortly after the bursts are observed. If the same burst is detected by *SWIFT* or *Fermi* and the GRID aboard the CubeSat, then the arrival time data of these gamma-bursts may be used to calculate the position of the CubeSat relative to the observatory (*SWIFT* or *Fermi*). Since the positions of both spacecraft will be known through other tracking means, the accuracy of this navigation method can be assessed by comparing the estimate of relative position to the known position of the CubeSat. Alternatively, the clock offset between the clock onboard the observatory and the clock on GRID could also be estimated.

Acknowledgment

The authors gratefully acknowledge the technical advice and support from the staff of ASTER Labs Inc. We also thank the NASA/Minnesota Space Grant Consortium for providing funding. Additionally, we would like to thank NASA's Balloon Program Office (BPO), the staff of NASA's Columbia Scientific Ballooning Facility, and Louisiana Space Grant Consortium for providing resources to test scientific space payloads. Lastly, the authors thank Kevin Hurley (Space Systems Laboratory, UC-Berkeley) and John Goldsten (Applied Physics Laboratory, Johns Hopkins University) for technical advice on detector design and experimental test procedures. While the authors gratefully acknowledge the aforementioned individuals and organizations, the views and conclusions expressed in this report are those of the authors alone and should not be interpreted as necessarily representing the official policies, either expressed or implied, of any organization.

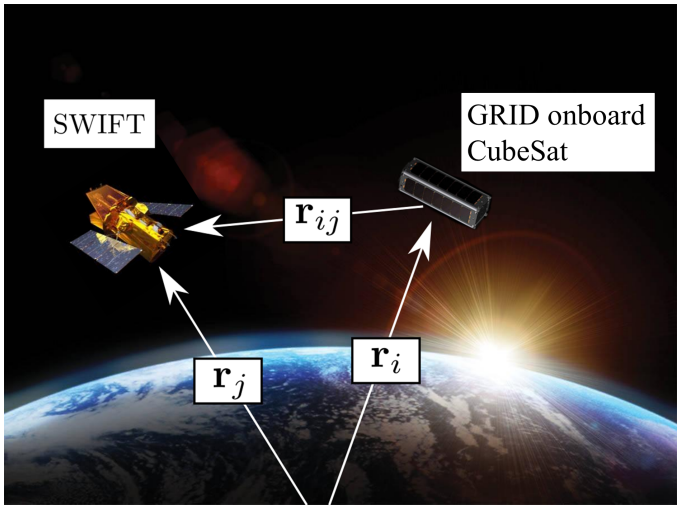

Fig. 9: Operation of GRID onboard a CubeSat, cooperating with other gamma-ray observatories

References

[1] NASA, "NASA Technology Roadmaps - TA5 (2015)," NASA, Washington, D.C., 2015.

[2] C.S. Hisamoto and S.I. SHeikh, "Spacecraft Navigation Using Celestial Gamma-Ray Sources," Journal of Guidance, Control, and Dynamics, vol. 38, pp. 1765-1774, 2015

[3] "Gamma Rays". NASA.

[4] T.H. Prettyman, W.C. Feldman, K.R. Fuller, S.A. Storms, S.A. Soldner, C. Szeles, F. P. Ameduri, D.J. Lawrence, M.C. Browne, and C.E. Moss, "CdZnTe Gamma Ray Spectrometer for Orbital Planetary Missions", Nuclear Science Symposium Conference Record, 2001 IEEE.

[5] P. T. Doyle, D. Gebre-Egziabher and S. I. Sheikh, "The Use of Small X-ray Detectors For Deep Space Relative Navigation," in SPIE Nanophotonics and Macrophotonics for Space Environments, San Diego, 2012.

[6] Misra, P. and Enge, P., "Global Positioning System: Signals, Measurements, and Performance," 2nd, Ganga-Jamuna Press, 2006.

[7] Hamamatsu Photonics, "Si APD S8664 series"

[8] Emadzadeh, A.A., Speyer, J.L., "Asymptotically Efficient Estimation of Pulse Time Delay For X-ray Pulsar Based Relative Navigation".

[9] C. H. Knapp and G. C. Carter, "The generalized correlation method for estimation of time delay," IEEE Trans. Acoustics, Speech, and Signal Processing, vol. ASSP-24, pp. 320-327, Aug. 1976.

[10] Zhang and Wu, "On Cross Correlation Based Discrete Time Delay Estimation," Department of Electrical and Computer Engineering McMaster University, Hamilton, Ontario, Canada, L8S 4K1.

[11] Leo, W. R. 1992, Techniques for Nuclear and Particle Physics Experiments: A How-to Approach (Berlin: Springer).

[12] Jacovitti and Scarano, "Discrete Time Techniques for Time Delay Estimation," IEEE Transactions on Signal Processing (Impact Factor: 2.79). 03/1993; 41(2):525 - 533. DOI: 10.1109/78.193195.

[13] http://laspace.lsu.edu/hasp/groups/Payload.php?py=2015&pn=03

[14] "Next Generation Communications." NASA Goddard Space Flight Center tech sheets, http://gsfctechnology.gsfc.nasa.gov/TechSheets/XRAY_Goddard_Final.pdf

[15] Sheikh, Suneel, I., et al, "Absolute and Relative Position Determination Using Variable Celestial X-ray Sources." 30th Annual AAS Guidance and Control Conference, 2007, Breckenridge, CO.

[16] Hanson, John, et. al, "Noise Analysis for X-ray Navigation Systems." IEEE-ION PLANS, May 2008.

[17] Peterson, L.E., et. al, "Techniques in Balloon X-ray Astronomy." Space Science Reviews, 13:320-336, 1972.